

# Angiotensin II, hypertension and angiotensin II receptor antagonism: Roles in the behavioural and brain pathology of a mouse model of Alzheimer's disease

Maximilian Wiesmann<sup>1,2</sup>, Monica Roelofs<sup>1</sup>,  
Robert van der Lugt<sup>1</sup>, Arend Heerschap<sup>3</sup>,  
Amanda J Kiliaan<sup>1,\*</sup> and Jurgen AHR Claassen<sup>2,\*</sup>

## Abstract

Elevated angiotensin II causes hypertension and contributes to Alzheimer's disease by affecting cerebral blood flow. Angiotensin II receptor blockers may provide candidates to reduce (vascular) risk factors for Alzheimer's disease. We studied effects of two months of angiotensin II-induced hypertension on systolic blood pressure, and treatment with the angiotensin II receptor blockers, eprosartan mesylate, after one month of induced hypertension in wild-type C57bl/6j and A $\beta$ PPswe/PS1 $\Delta$ E9 (A $\beta$ PP/PS1/Alzheimer's disease) mice. A $\beta$ PP/PS1 showed higher systolic blood pressure than wild-type. Subsequent eprosartan mesylate treatment restored this elevated systolic blood pressure in all mice. Functional connectivity was decreased in angiotensin II-infused Alzheimer's disease and wild-type mice, and only 12 months of Alzheimer's disease mice showed impaired cerebral blood flow. Only angiotensin II-infused Alzheimer's disease mice exhibited decreased spatial learning in the Morris water maze. Altogether, angiotensin II-induced hypertension not only exacerbated Alzheimer's disease-like pathological changes such as impairment of cerebral blood flow, functional connectivity, and cognition only in Alzheimer's disease model mice, but it also induced decreased functional connectivity in wild-type mice. However, we could not detect hypertension-induced overexpression of A $\beta$  nor increased neuroinflammation. Our findings suggest a link between midlife hypertension, decreased cerebral hemodynamics and connectivity in an Alzheimer's disease mouse model. Eprosartan mesylate treatment restored and beneficially affected cerebral blood flow and connectivity. This model could be used to investigate prevention/treatment strategies in early Alzheimer's disease.

## Keywords

Alzheimer's, brain imaging, cerebral blood flow, cognitive impairment, hypertension

Received 9 May 2016; Revised 26 July 2016; Accepted 8 August 2016

## Introduction

Dementia has become a public health problem in the aging world population.<sup>1,2</sup> Alzheimer's disease (AD) and vascular dementia (VaD) are the number one and two disorders, together responsible for most cases of dementia.<sup>3,4</sup> Epidemiological and clinical studies revealed that AD and VaD share common vascular-related risk factors such as hypertension, diabetes, hyperlipidemia, cerebrovascular disease, and arrhythmia.<sup>5–12</sup> Of these, hypertension is the most common cardiovascular risk

<sup>1</sup>Department of Anatomy, Radboud Alzheimer Center, Donders Institute for Brain, Cognition & Behaviour, Radboud university medical center, Nijmegen, The Netherlands

<sup>2</sup>Department of Geriatric Medicine, Radboud Alzheimer Center, Donders Institute for Brain, Cognition & Behaviour, Radboud university medical center, Nijmegen, The Netherlands

<sup>3</sup>Department of Radiology & Nuclear Medicine, Radboud university medical center, Nijmegen, The Netherlands

\*These authors share last authorship.

## Corresponding author:

Jurgen AHR Claassen, Department of Geriatric Medicine, Radboud Alzheimer Center, Donders Institute for Brain, Cognition & Behaviour, Radboud university medical center, P.O. Box 9101, Nijmegen 6500 HB, The Netherlands.

Email: Jurgen.Claassen@Radboudumc.nl

factor for dementia. In coming years, the expected increase in the prevalence of hypertension due to the aging world population could also raise the number of AD patients, since midlife and late-life hypertension almost double the risk of developing AD in later life.<sup>13,14</sup> Whether this association between hypertension and AD is causal – and if so, through which mechanism – remains unknown.

Angiotensin II (AngII), a component of the renin-angiotensin system (RAS), is a candidate for the hypothesised mechanistic link between hypertension and AD.<sup>15</sup> AngII has a prominent role in blood pressure (BP) regulation,<sup>16</sup> causing vasoconstriction and elevated BP by binding to the AngII-receptor type1 (AGTR1) and type2 (AGTR2),<sup>16,17</sup> and is considered to be a key mediator of the clinical syndrome of essential hypertension,<sup>18</sup> through chronically induced vasoconstriction, increased aldosterone secretion, increased sympathetic tone, and cardiac and vascular hypertrophy.<sup>19,20</sup>

How could AngII be linked mechanistically to AD? When initiated during midlife, chronically elevated levels of AngII, in addition to causing hypertension, may induce cerebral vascular dysfunction by promoting vascular remodelling and inflammation,<sup>16,21</sup> causing malfunctioning of the neurovascular unit,<sup>22,23</sup> and promoting expression of amyloid- $\beta$  precursor protein (A $\beta$ PP) and A $\beta$  production.<sup>23</sup>

Preclinical data show that cerebrovascular dysfunction is partly caused by AngII directly, and not via elevated BP alone.<sup>24</sup> A decreased cerebral blood flow (CBF) is an important and consistent early feature of AD, possibly as result of the accumulation of A $\beta$  in or close to blood vessels.<sup>25–27</sup> Another hallmark of AD is a reduced glucose metabolism particularly in the temporal and parietal cortex.<sup>28,29</sup> Being selectively highly expressed in the capillary endothelium of the brain, glucose transporter type 1 (GLUT-1) is responsible for transfer of glucose across the blood-brain barrier.<sup>30</sup> A decreased hippocampal and cortical amount of GLUT-1 has been revealed in the brains of AD patients.<sup>31–33</sup> Another important component of AD pathology is neuroinflammation, manifested by activation of microglia.<sup>34–36</sup> Ionised calcium-binding adapter molecule 1 (IBA-1) is a marker for active and resting microglia.<sup>37–39</sup> GLUT-1 and IBA-1 are used in this study as markers for changes in metabolism, vascular density, and neuroinflammation.

Further support for this mechanistic link between AngII and AD comes from recent clinical trials and studies in animal models showing that AD pathology can be reduced via RAS.<sup>40–43</sup>

AngII receptor blockers (ARBs) specifically inhibit the activation of AGTR1 and thus the actions of AngII.<sup>41</sup> Preclinical and clinical studies indicate that antihypertensives may reduce the development of

AD.<sup>44,45</sup> Specifically, ARBs have been associated with a reduced risk of AD.<sup>46,47</sup> Findings from the Observational Study on Cognitive function and SBP Reduction (OSCAR) suggest that Eprosartan (ARB) is associated with preservation or improvement of cognitive performance.<sup>48</sup> A case-control analysis showed that patients on ARBs and ACE-Is had a respectively 53% and 24% reduced risk of AD, compared to patients on other antihypertensives.<sup>46</sup>

If indeed AngII is a causal factor linking hypertension to AD, we hypothesise three potential mechanisms: (1) AngII initiates A $\beta$  accumulation through increased production and/or reduced clearance, leading to AD pathology; (2) A $\beta$  accumulation is initiated by other factors, but AngII contributes to AD by enhancing cerebrovascular toxicity and inflammatory potency of A $\beta$ , and/or by contributing to enhanced A $\beta$  production or reduced A $\beta$  clearance; (3) AngII leads to neurovascular dysfunction causing cognitive decline independent of AD pathology, but adding to the cognitive effects of AD or even mimicking AD in absence of underlying AD pathology.

To investigate these hypotheses, we developed a translational animal model to study the following mechanisms: (1) Can AngII induce AD-related pathology in wild-type (WT) mice; (2) Can AngII exacerbate AD pathology in the A $\beta$ PP/PS1 mouse model for AD; (3) Can AngII induce cerebrovascular, metabolic/inflammatory, and/or functional connectivity (FC) changes that mimic AD in WT animals or that add to the effects of AD pathology in A $\beta$ PP/PS1 mice. In addition, to uncover the effects of AngII on AD, we aim to investigate whether treatment with the AngII receptor antagonist eprosartan mesylate (EM) is able to prevent or reduce AngII-induced changes. The overall aim of this study is to elucidate the mechanisms through which hypertension and antihypertensive treatment influence AD. Translational characteristics of this study are the exposure to AngII at 10 months to simulate midlife hypertension, inclusion of WT animals in addition to transgenic animals to better translate to sporadic AD, and the use of magnetic resonance imaging (MRI) techniques with protocols similar to those used in clinical studies. We use flow-sensitive alternating inversion recovery-arterial spin labeling (FAIR-ASL) to measure changes in CBF and diffusion tensor imaging (DTI) to reveal pathological adaptations in microstructural integrity of the white matter (WM) and grey matter (GM). Several studies have revealed decreases in CBF in AD compared to healthy controls such as prefrontal cortex,<sup>49</sup> temporo-occipital and parieto-occipital association cortices,<sup>50</sup> and hippocampus.<sup>51</sup> Mean diffusivity (MD) is a measure of DTI which increases in presence of tissue damage.<sup>52</sup> Previous studies demonstrated an increased MD not only in frontal<sup>53,54</sup> and temporal

lobes,<sup>53–58</sup> but also in intercerebral tracts, including the superior superior longitudinal fasciculus<sup>59</sup> and the corpus callosum.<sup>54</sup>

## Materials and methods

### Animals

The A $\beta$ PP<sub>swc</sub>/PS1<sub>dE9</sub> (A $\beta$ PP/PS1) founder mice were originally obtained from John Hopkins University, Baltimore, MD, USA (D. Borchelt and J. Jankowsky, Department of Pathology),<sup>60,61</sup> and a colony is bred at the Central Animal Facility at Radboud University Medical Center, The Netherlands. This line was originally maintained on a hybrid background by backcrossing to C3HeJ $\times$ C57BL/6J F1 mice, and for the present work, the breeder mice were backcrossed to C57BL/6J for 15 generations to obtain mice for the current study. Before the actual experiments, animals were housed socially with a maximum of six animals per cage, with room temperature at 21°C, and artificial 12:12 h light:dark cycle (lights on at 7 a.m.). Throughout the experiments, the mice were housed separately after the micro-osmotic pump implantation to control intake of drinking water or water mixed with medication. Food and water were available *ad libitum*.

We used 51 10-month-old male mice (29 WT littermates and 22 A $\beta$ PP/PS1 mice); at 12 months of age, all animals completed the experiments and were euthanised. All experiments were performed between 8 a.m. and 6 p.m.

### Study design, randomisation, and blinding

This was a randomised and controlled assessor-double-blind study. The experiments were performed according to the Dutch federal regulations for animal protection and approved (WP130084 + RU-DEC 2013-001) by the Veterinary Authority of Radboud University Medical Center, Nijmegen, The Netherlands and the Animal Experiment Committee of the Radboud University, Nijmegen, The Netherlands. The reporting of the animal experiments is according to ARRIVE guidelines.<sup>62</sup> Per experimental subgroup, the selection of animals was randomised. There was no increased mortality ( $n = 0$ ) in this study. For the sample size calculation and ranked experimental outcomes per research question, see the supplementary materials. The A $\beta$ PP/PS1 and WT mice were split in two main groups: (1) induced hypertension (using AngII-infusion delivered by subcutaneously implanted micro-osmotic pumps) and (2) controls (saline infusion, further called Sal-infused animals/ mice). Supplemental Table 1 provides an overview of the study design and number of animals per group. No animals were excluded from analysis. After

one month, both animal groups on AngII or saline infusion were further divided into two subgroups: treatment with EM (ARB) and standard drinking water as control. At age 10 and 11 months, systolic BP (SBP) was measured. Morris water maze (MWM) was exerted at 11 months. MRI measurements were performed at the age of 12 months. Post mortem immunohistochemical and biochemical procedures were performed.

### Micropumps implantation and tail-cuff plethysmography

The implantation of the micro-osmotic pumps (ALZET, CA, USA, model 1004) to deliver either AngII (500 ng $\cdot$ kg<sup>-1</sup> $\cdot$ min<sup>-1</sup>, Sigma-Aldrich, Missouri, USA) or sterile saline (Sigma-Aldrich, Missouri, USA) and the tail-cuff plethysmography (IITC Life Scientific Instruments, Woodland Hills, CA) were performed, as previously described.<sup>63</sup>

### Drug treatment

To investigate the effects of an AngII receptor antagonist, mice were supplemented with EM (Sigma-Aldrich, Missouri, USA) dissolved in drinking water for four weeks (0.35 mg $\cdot$ kg<sup>-1</sup> $\cdot$ day<sup>-1</sup>), like previously described.<sup>63</sup>

### Morris water maze

Spatial learning and memory were tested in the MWM (for more detailed information, see Janssen et al.<sup>64</sup>).

### MRI protocol

MRI measurements were performed, as previously described.<sup>65</sup> For the imaging procedure, the animals were anaesthetised with isoflurane (3.5% for fast induction and 1.7% for maintenance) in a 2:1 oxygen and N<sub>2</sub>O mixture (normal gas condition) or in a 3:0 oxygen and N<sub>2</sub>O mixture (vasoconstriction) with an air flow of 300 mL/min, and placed in a stereotactic holder to prevent movement during the scanning. Body temperature was monitored with a rectal temperature probe and maintained at 37°C with heated airflow. Respiration of the animal was monitored using a pneumatic cushion respiratory monitoring system (Small Animal Instruments Inc, NY, USA). First gradient echo T2\*-weighted images covering the entire mouse brain were acquired in three directions for anatomical reference using previously described image parameters.<sup>66</sup>

### Cerebral blood flow

MR perfusion data were measured with FAIR MRI techniques; from a series of echo planar imaging

(EPI), images in three different regions of interest (ROI) were evaluated<sup>67,68</sup> in the cerebral cortex (all cortical regions above corpus callosum), hippocampus, thalamus according to the Paxinos and Franklin atlas.<sup>69</sup> Regional CBF was calculated as described earlier.<sup>66</sup>

### Diffusion tensor imaging

Diffusion of water was imaged as described previously.<sup>70,71</sup> Mean water diffusivity (MD) and fractional anisotropy (FA) were derived from the tensor estimation following a protocol as described elsewhere.<sup>71</sup> MD and FA values were measured in several WM and GM areas, manually selected based on an anatomical atlas.<sup>69</sup>

### Resting-state fMRI

Subsequently after the acquisition of the anatomical reference images, resting-state fMRI (rsfMRI) datasets were acquired using a single-shot spin-echo sequence combined with EPI (SE-EPI) sequence in anaesthetised mice, as published previously.<sup>65</sup> FC group comparison between ROIs (left and right dorsal hippocampus, left and right ventral hippocampus, left and right auditory cortex, left and right motor cortex, left and right somatosensory cortex, and left and right visual cortex) were calculated from the blood oxygen level dependent (BOLD) time series using total correlation analyses implemented in FSLNets (FSLNets v0.3; www.fmrib.ox.ac.uk/fsl), using previously published protocol.<sup>65</sup> Pearson's correlation values were Fisher transformed to Z-scores for group comparisons and statistical analysis.

### Immunohistochemical procedures

After scanning, the mice were sacrificed by transcardial perfusion using 0.1 M phosphate-buffered saline (PBS). Details on tissue preparation and sectioning are described earlier.<sup>71</sup>

A triple fluorescent staining for glucose transporter-1 (GLUT-1), IBA-1, and A $\beta$  was performed on free-floating brain sections on shaker tables at room temperature. Brain sections were first rinsed with 0.1 M PBS and pre-incubated in 0.5 mL 0.1 M PBS-BT for 30 min. After pre-incubation, primary antibodies (A $\beta$ : Mouse anti-human-A $\beta$  1:10000; WO-2 antibody, mouse anti-human A $\beta$ 4-10, T Hartmann, Heidelberg, Germany), IBA-1: Goat anti-IBA-1 (1:750; Abcam, Cambridge, UK), and GLUT-1: Rabbit anti-GLUT-1 (1:5000; Millipore, Billerica, MA, USA) were added for 16 h. All sections were rinsed and the secondary antibodies (A $\beta$ : Alexa647-conjugated donkey anti-mouse IgG, IBA-1: Cy3-conjugated donkey anti-goat IgG,

GLUT-1: Alexa 488-conjugated donkey anti-Rabbit IgG; Jackson ImmunoResearch Inc, Allentown, PA, USA) was added for 3 h in the dark. After rinsing, mounting, and drying sections were enclosed with Fluorsave (Calbuichem, Canada).

### Quantification

Brain sections between bregma  $-1.46$  and  $-2.30$ <sup>69</sup> were preselected for quantification. Quantification was done at a  $5\times$  magnification using an Axio Imager (A2, Zeiss Germany). ImageJ (National Institute of Health, Bethesda, MD, USA) was used to analyse the ROI (cortex, hippocampus, and thalamus).

### Statistics

For statistical analyses, IBM SPSS Statistics 20 software was used (IBM Corporation, New York, NY, USA).

We first analysed data gathered under untreated conditions (no EM). To unravel the impact of AngII-induced hypertension on all parameters and the possible genotype by AngII-induced hypertension interactions, data were analysed separately with univariate/multivariate analysis of variance (ANOVA) with Bonferroni correction.

To assess effects of treatment (EM), data were analysed separately for AngII-infused and Sal-infused animals with univariate/multivariate ANOVA with Bonferroni correction for multiple comparisons. After overall analysis, data were split into the specific interacting factors, when significantly different.

The repeated measures ANOVA with Bonferroni correction was only used for the acquisition phase of the MWM (with the repeated measure: acquisition days/time). All values of the MWM acquisition are expressed as mean  $\pm$  SEM for. All other results are shown in box plots with whiskers. The hinges of the boxes extend from the 25th to 75th percentiles of the data. The whiskers are drawn down to the 5th percentile and up to the 95th. For all statistical analyses, there are significant comparisons between groups and treatments over all experimental outcome measures, and Type I error was consistently controlled and limited to  $p \leq 0.05$  overall.

### Results

Body weight was not influenced by genotype, AngII-infusion nor treatment with EM before (10 months), and during the experiment (11 and 12 months) (Figure 1(a)).

At 11 months of age, AngII-infused mice, both A $\beta$ PP/PS1 and WT mice, drank daily more water

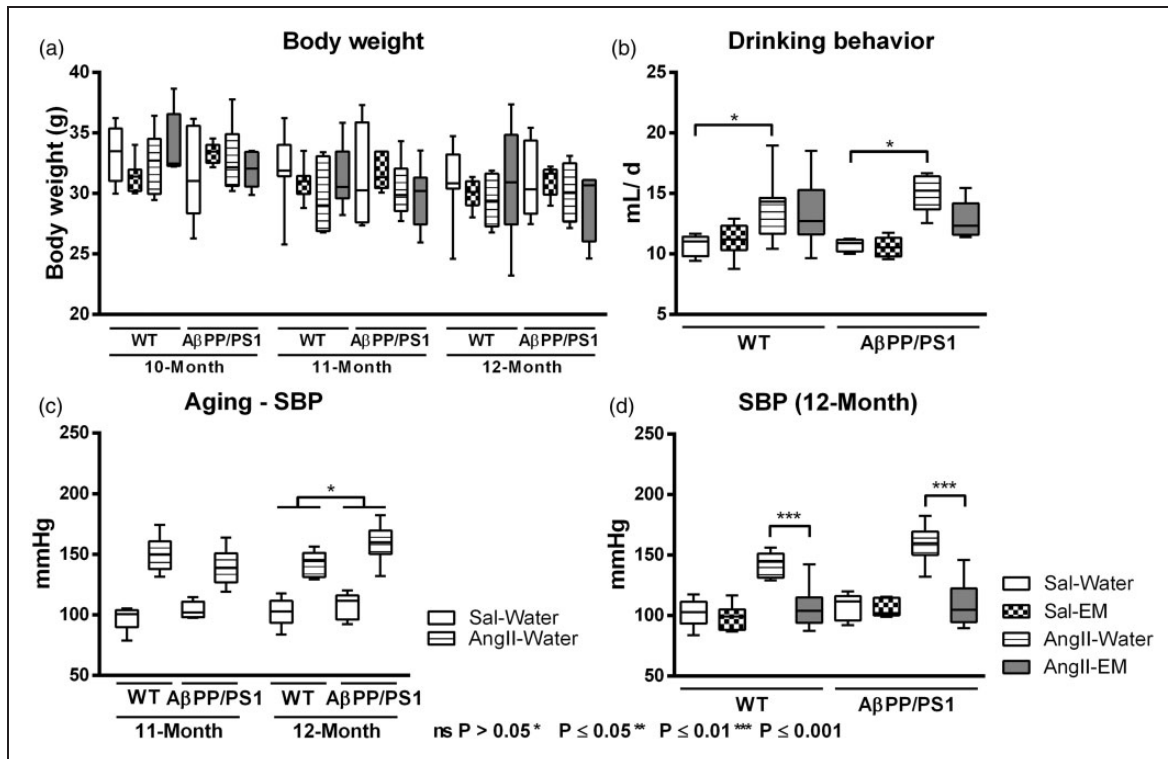


**Figure 1.** Effect of aging, angiotensin II (AngII)-infusion, and treatment with eprosartan mesylate (EM) on body weight (a), drinking behaviour (b), systolic blood pressure (c+d, SBP) of AβPP/PS1, and wild-type (WT) mice treated with EM versus water as control. (a) No significant genotype, AngII, or EM effects were observed on body weight. (b) AngII-infusion increased water intake both in untreated AβPP/PS1 and WT ( $p = 0.012$ ) compared to their corresponding control Sal-infused (saline) littermates. This effect was not influenced by genotype or treatment with EM in AngII-infused and Sal-infused animals. (c) SBP was measured for two consecutive days in trained, conscious, and preheated mice using computerised tail-cuff plethysmography. During both experimental months, infusion with AngII effectively increased SBP (11 months:  $44.6 \pm 4.8$  mmHg; 12 months:  $45.5 \pm 4.9$  mmHg) in all mice compared to littermates without AngII (11 months,  $p < 0.001$ ; 12 months,  $p < 0.001$ ). At 12 months of age, untreated (no EM) Sal-infused and AngII-infused AβPP/PS1 mice had a higher SBP than their corresponding WT mice ( $11.4 \pm 4.9$  mmHg;  $p = 0.030$ ). (d) Only in AngII-infused animals, not in Sal-infused animals, treatment with EM lowered SBP ( $-42.5 \pm 6.5$  mmHg;  $p < 0.001$ ).

than Sal-infused mice (Figure 1(b),  $F(1,22) = 7.5$ ,  $p = 0.012$ ).

### Systolic blood pressure

**Aging by genotype interactions on the relationship between AngII and SBP.** Repeated measures ANOVA revealed a genotype by AngII interaction on SBP ( $p = 0.032$ ) over time (Figure 1(c)).

AngII effectively increased SBP (11 months:  $44.6 \pm 4.8$  mmHg; 12 months:  $45.5 \pm 4.9$  mmHg) in all mice compared to littermates without AngII at 11 and 12 months of age (11 months,  $F(1,22) = 85.0$ ,  $p < 0.001$ ; 12 months,  $F(1,22) = 85.6$ ,  $p < 0.001$ ).

At 12 months of age, all AβPP/PS1 mice had a higher SBP than corresponding WT ( $11.4 \pm 4.9$  mmHg;  $F(1,22) = 5.4$ ,  $p = 0.030$ ).

**AngII, antihypertensive treatment with EM, and SBP.** At 12 months of age, EM treatment lowered SBP (Figure

1(d);  $-42.5 \pm 6.5$  mmHg;  $F(1,22) = 42.8$ ,  $p < 0.001$ ) only in AngII-infused animals, and not in Sal-infused animals.

### Cerebral blood flow

One representative high-resolution voxel-wise analysed CBF image is shown in Figure 2(a). At 12 months of age, CBF was measured in the cortex (Figure 2(b)), hippocampus (Figure 2(c)), and thalamus (Figure 2(d)).

Furthermore, CBF was acquired in two standardised gas concentrations: normal (200 O<sub>2</sub>: 100 N<sub>2</sub>O mL/min) and vasoconstriction (300 O<sub>2</sub>: 0 N<sub>2</sub>O mL/min). For each ROI (cortex, hippocampus, thalamus) and each gas concentration (normal (200 O<sub>2</sub>: 100 N<sub>2</sub>O mL/min) and vasoconstriction (300 O<sub>2</sub>: 0 N<sub>2</sub>O mL/min)), data were analysed on one hand to detect genotype effects on the relationship between AngII and CBF, and on the other hand to investigate the relationship between AngII, antihypertensive treatment with EM, and CBF.

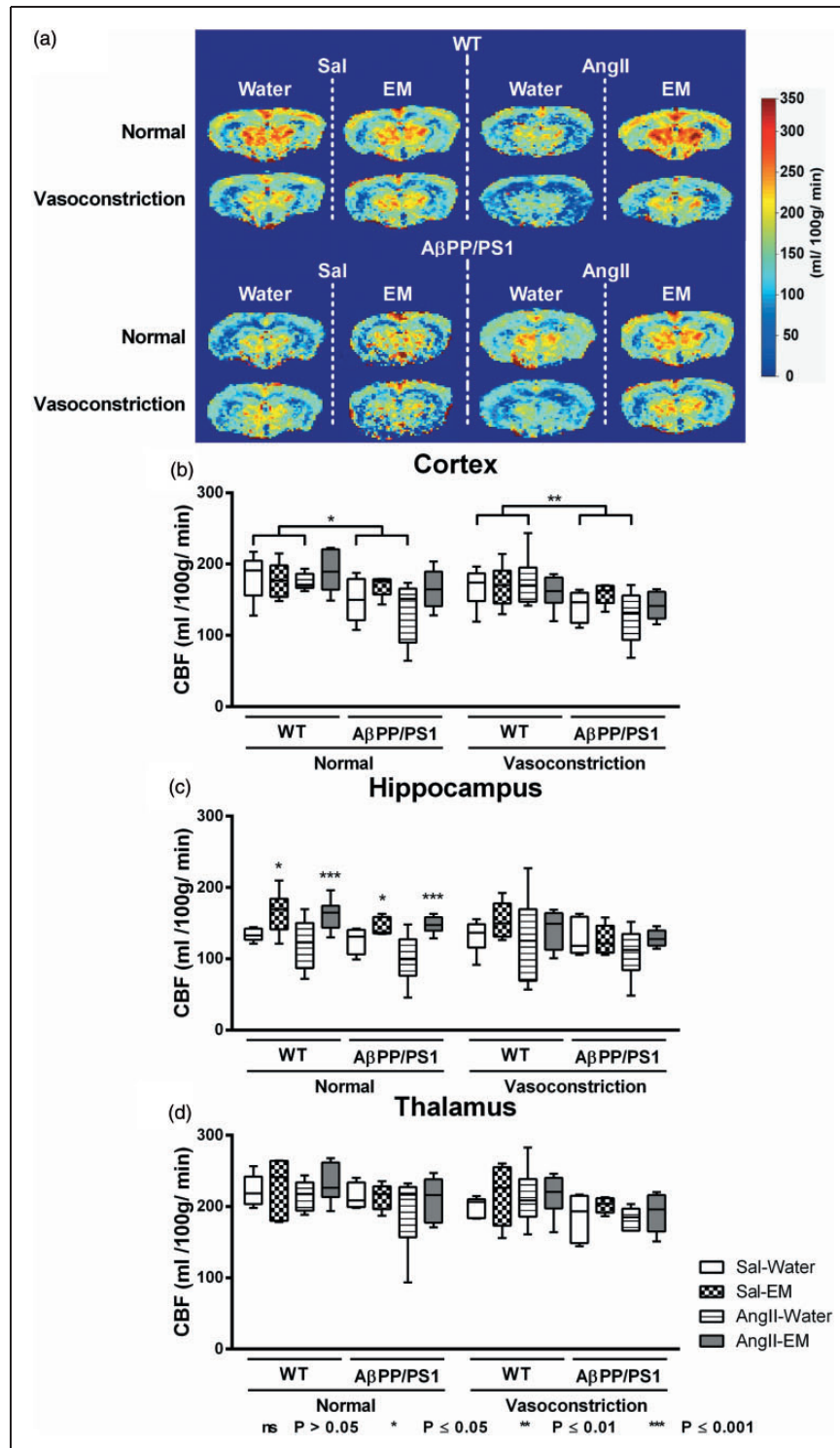


**Figure 2.** Cerebral blood flow (CBF) measurements of the brains of 12-month-old saline-infused (Sal) and Angiotensin II-infused (AngII) AβPP/PS1 and wild-type (WT) mice, treated with eprosartan mesylate (EM) vs. normal drinking water as control. CBF was measured with flow-sensitive alternating inversion recovery MRI technique, from a series of echo planar imaging images. One representative high-resolution voxel-wise analysed CBF image for each single animal group is shown (a). The figure shows the cerebral perfusion data of AβPP/PS1 and WT mice infused with either saline (sal) or angiotensin II (AngII) and treated with either eprosartan mesylate (EM) compared to water as control. The CBF was measured in three different regions of interest (ROI): Cortex (b), hippocampus (c), and thalamus (d). (b) Under normal gas concentration (normoxia = 2:1 O<sub>2</sub> and N<sub>2</sub>O mixture) all untreated (no EM) AβPP/PS1 mice exhibited a decreased cortical CBF compared to their corresponding WT littermates ( $p = 0.012$ ). Again, under gas concentration inducing vasoconstriction (3: O<sub>2</sub> and N<sub>2</sub>O mixture), all untreated (no EM) AβPP/PS1 mice demonstrated a decreased cortical CBF compared to their corresponding WT littermates ( $p = 0.009$ ). (c) Under normal gas concentration, Treatment with EM increased hippocampal CBF both in AngII- ( $p = 0.001$ ) and Sal-infused ( $p = 0.012$ ) animals compared with untreated (no EM) animals.

**Cortex.** Normal gas condition: A $\beta$ PP/PS1 mice had a lower cortical CBF than WT littermates ( $-36.7 \pm 13.2$  mL/100 g/min;  $F(1,19) = 7.7$ ,  $p = 0.012$ ).

Gas condition inducing vasoconstriction: A $\beta$ PP/PS1 mice had a decreased cortical CBF compared to corresponding WT littermates ( $-38.5 \pm 13.1$  mL/100 g/min;  $F(1,19) = 8.6$ ,  $p = 0.009$ ).

**Hippocampus.** Normal gas condition: Treatment with EM increased hippocampal CBF both in AngII- ( $44.5 \pm 10.9$  mL/100 g/min;  $F(1,21) = 16.5$ ,  $p = 0.001$ ) and Sal-infused ( $25.5 \pm 9.0$  mL/100 g/min;  $F(1,16) = 8.0$ ,  $p = 0.012$ ) animals compared with untreated (no EM) animals.

Gas condition inducing vasoconstriction: No significant differences were found.

**Thalamus.** Normal gas condition: No significant differences were found.

Gas condition inducing vasoconstriction: No significant differences were found.

### Diffusion tensor imaging

In this study, brain diffusivity determined with DTI is a measure for white and GM integrity. One DTI measure is FA being a marker for myelination and fibre density of WM and MD represents an inverse measure of membrane density, and sensitive measure for cellularity, oedema, and necrosis in GM.<sup>72–74</sup>

Quantitative assessment of diffusion tensor-derived indices was performed for ROIs drawn in white and grey matter regions (Figure 3(a)) to assess effects of AngII-induced hypertension and genotype in 12-month-old A $\beta$ PP/PS1 and WT mice (Figure 2(b) and (c)). Moreover, in AngII-infused and Sal-infused mice, the impact of antihypertensive treatment with EM on microstructural integrity in white and GM regions was measured.

**Fractional anisotropy.** Treatment with EM led to higher hippocampal FA in all AngII-infused animals (transgenic and WT) ( $F(1,18) = 5.0$ ,  $p = 0.039$ ), also in the optic tract ( $F(1,17) = 12.9$ ,  $p = 0.002$ ) compared to animals without EM.

**Mean diffusivity.** EM treatment decreased MD in the motor cortex of all Sal-infused mice ( $F(1,13) = 8.0$ ,  $p = 0.014$ ) compared to Sal-infused mice without EM. Only in AngII-infused animals, a genotype by EM interaction was detected for MD in motor cortex ( $p = 0.036$ ) and optic tract ( $p = 0.008$ ).

In detail, non-EM-treated AngII-infused A $\beta$ PP/PS1 mice showed lower MD in the optic tract compared to WT ( $F(1,8) = 7.4$ ,  $p = 0.026$ ).

However, on EM treatment, the MD in the motor cortex of AngII-infused A $\beta$ PP/PS1 mice was decreased compared to the non-treated mouse ( $F(1,9) = 6.4$ ,  $p = 0.033$ ). In AngII-infused EM-treated WT, a decreased MD in the optic tract was found compared to the non-treated mouse ( $F(1,8) = 6.4$ ,  $p = 0.035$ ).

### Resting-state fMRI

rsfMRI is based on the principle that during the resting state in functionally related brain regions spontaneous low-frequency fluctuations ( $<0.08$  Hz) of the BOLD signals occur synchronously implying a possible neuronal FC. Li et al.<sup>75</sup> showed that AD patients have a different FC including alterations in the visual, sensory motor, and visual networks. Therefore, we also included these ROI (visual, motor, and somatosensory cortex) in our analysis. To compare FC patterns in 12-month-old mice (Figure 4), rsfMRI data were analysed for genotype and AngII effects in untreated animals. In addition, in AngII-infused and Sal-infused mice, the effect of antihypertensive treatment with EM on FC was investigated.

**Total correlation analyses.** A $\beta$ PP/PS1 showed no differences in FC compared to their WT littermates.

Notably, in both A $\beta$ PP/PS1 and WT mice, AngII-induced hypertension led to a decreased FC between several brain regions, see supplementary Table 2.

Investigating the effect of antihypertensive treatment with EM on FC in AngII-infused and Sal-infused animals revealed only negative effects of EM in Sal-infused animals and only positive effects on the FC in AngII-infused animals. More specifically, Sal-infused mice treated with EM had a lower FC between several brain regions than Sal-infused mice not treated with EM, see supplementary Table 2. In contrast, AngII-infused mice on EM showed a higher FC than non-EM-treated AngII-infused mice between many brain regions, see supplementary Table 2.

### Morris water maze

All mice were trained in the water maze task to assess spatial learning capacity at 11 months of age (Figure 5). During task acquisition, the latency to reach the platform was assessed (Figure 5(a) to (c)). Spatial memory was measured with the probe trial 1 h after the last regular trial on the last day of the MWM experiment using the frequency of crossing the northeast quadrant containing the platform position (Figure 5(d)).

**Acquisition.** A genotype by AngII interaction was found for the latency to reach the platform in the acquisition phase (Figure 5(a),  $p = 0.009$ ). Sal-infused A $\beta$ PP/PS1

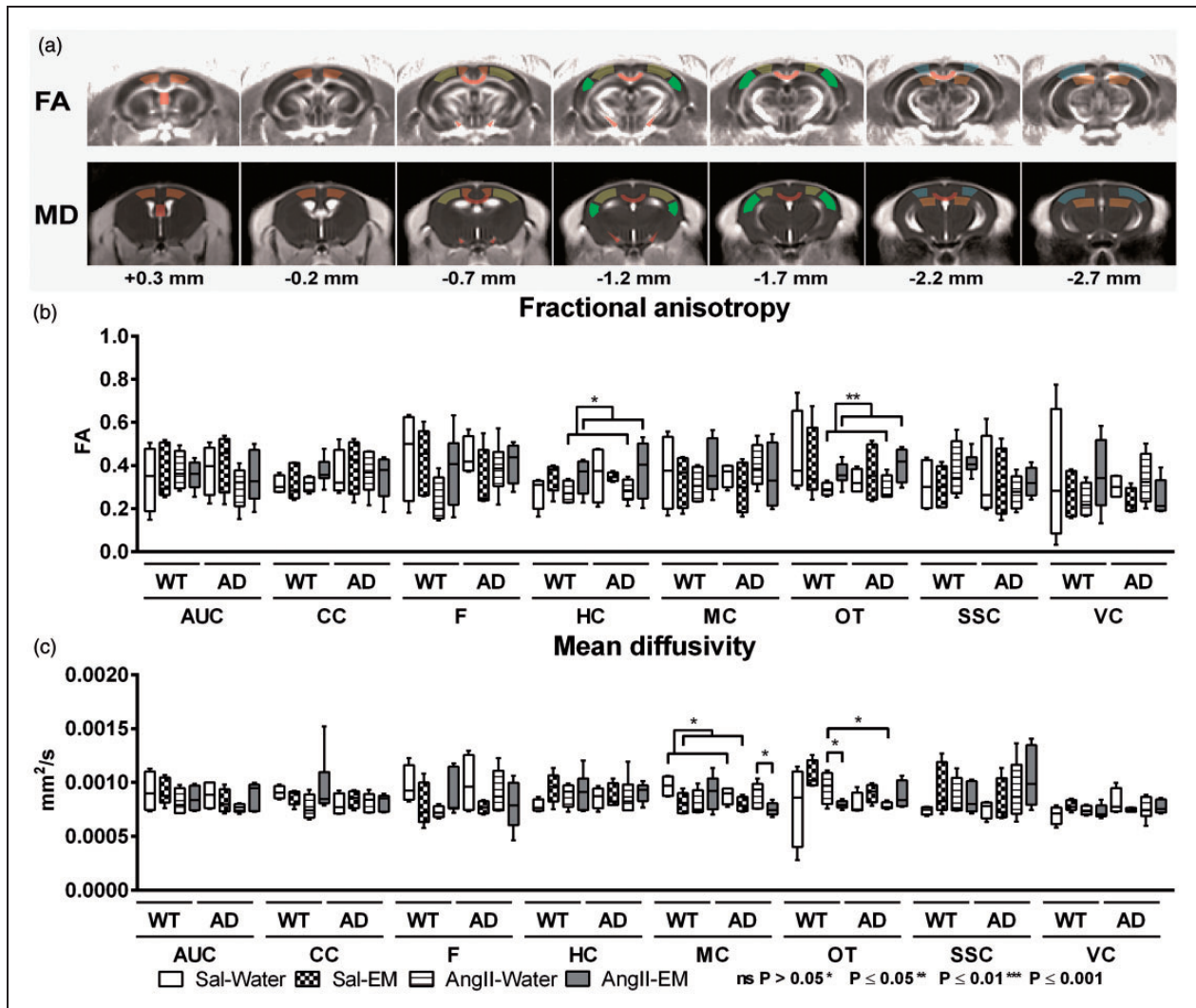


**Figure 3.** Diffusion tensor imaging (DTI) measurements of the brains of 12-month-old saline-infused (Sal) and Angiotensin II-infused (AngII) A $\beta$ PP/PS1 (Alzheimer's disease, AD) and wild-type (WT) mice, treated with eprosartan mesylate (EM) vs. normal drinking water as control. Quantitative assessment of diffusion tensor-derived indices was performed for regions of interest (ROI; AUC: auditory cortex; CC: corpus callosum; F: fornix; HC: hippocampus; MC: motor cortex; OT: optic tract; SSC: somatosensory cortex, VC: visual cortex). (a) ROIs were drawn in white and grey matter to assess effects of AngII-infusion (induced hypertension) and antihypertensive treatment with EM in 12-month-old A $\beta$ PP/PS1 and WT mice on fractional anisotropy (b) and mean diffusivity (c). (B) Under AngII-infusion, hippocampal FA ( $p = 0.039$ ) and FA in the optic tract ( $p = 0.002$ ) were higher if animals were treated with EM compared with AngII without EM. (c) In all Sal-infused mice, EM treatment decreased MD in the motor cortex ( $p = 0.014$ ). AngII-infused A $\beta$ PP/PS1 mice (no EM) had a lower MD in the optic tract than their WT littermates ( $p = 0.026$ ). However, on EM treatment MD in the motor cortex of AngII-infused A $\beta$ PP/PS1 mice was decreased compared to their non-treated littermates ( $p = 0.033$ ). Under AngII-infusion, WT mice on EM had a decreased MD in the optic tract compared to their untreated littermates (no EM) ( $p = 0.035$ ).

( $F(3,9) = 4.2$ ,  $p = 0.041$ ) and WT mice ( $F(3,24) = 5.4$ ,  $p = 0.006$ ), and also AngII-infused WT mice ( $F(3,18) = 5.9$ ,  $p = 0.005$ ) were able to learn to find the platform from acquisition day 1 to day 4, whereas AngII-infused A $\beta$ PP/PS1 mice ( $F(3,15) = 2.5$ ,  $p = 0.100$ ) did not learn to find the platform from acquisition day 1 to day 4. Combining EM-treated with untreated mice revealed no effect or a genotype by antihypertensive treatment interaction (Figure 5(b) and (c)).

**Probe.** We detected no effects of genotype, AngII-infusion, or antihypertensive treatment with EM (Figure 5(d)).

### Immunohistochemical procedures

To analyse effects of genotype and AngII in untreated animals, AngII-infused and Sal-infused mice and also the effect of an antihypertensive treatment with EM on metabolism, vascular density, neuroinflammation and amount of A $\beta$ , all brains were



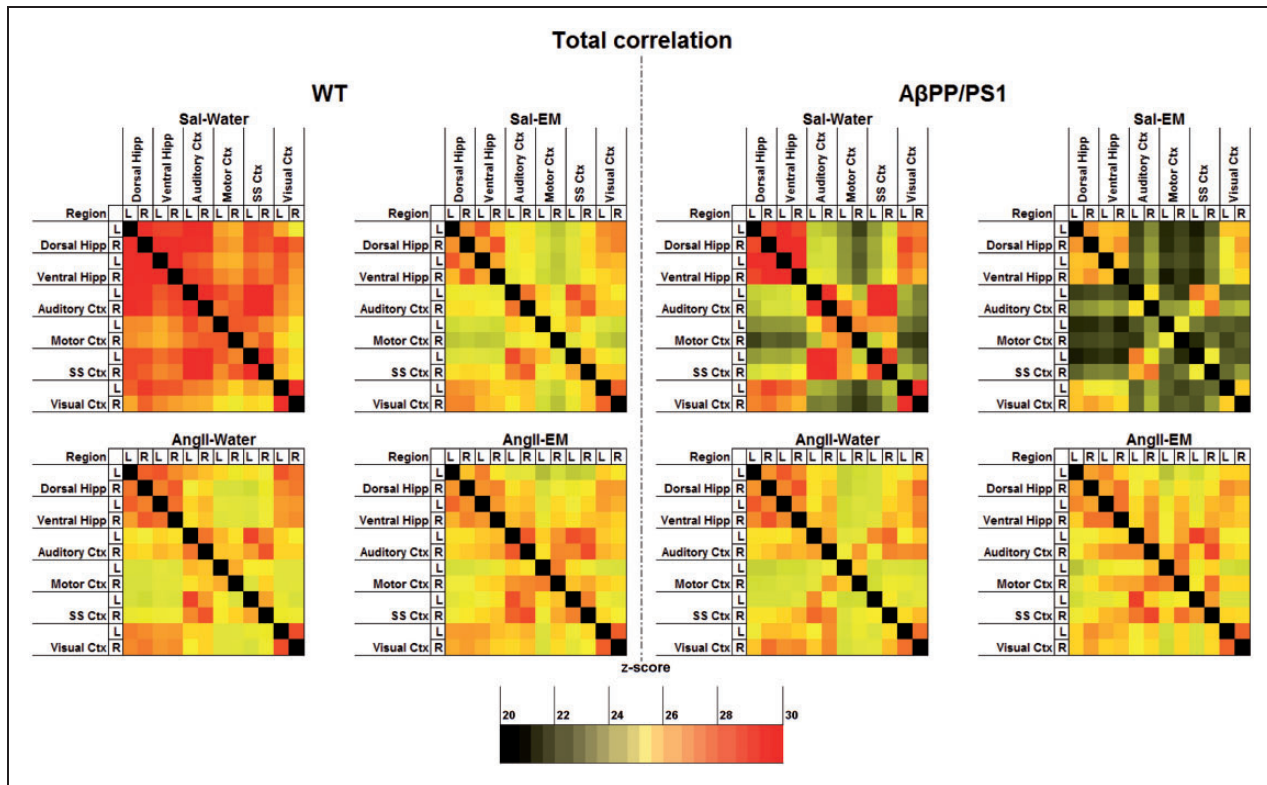


**Figure 4.** Resting-state functional connectivity (FC) based on total correlation analyses of 12 ROI in the brain of 12-month-old Sal-infused (saline) and AngII-infused (angiotensin II) A $\beta$ PP/PS1 and wild-type (WT) mice, treated with eprosartan mesylate (EM) vs. normal drinking water as control. In summary, for the overall correlations, no significant genotype effects were detected in the dorsal and ventral hippocampus (hipp), and auditory, motor, somatosensory (SS) and visual cortex (ctx) of untreated animals (no EM). Notably, in all mice, A $\beta$ PP/PS1 and WT mice, AngII-induced hypertension led to a decrease in FC between several brain regions, i.e. left dorsal hippocampus to right ventral hippocampus, left ventral hippocampus to left visual cortex, and right auditory ctx to right motor ctx. Investigating the effect of antihypertensive treatment with EM on FC in AngII-infused and Sal-infused animals revealed only negative effects of EM in normotensive animals and only positive effects on the FC in AngII-infused animals. A detailed description of the effects found in the total correlation analyses of the resting-state FC data is given in supplementary Table 2.

stained for glucose transporter-1 (GLUT-1), against IBA-1 and WO-2 antibody (mouse anti-human A $\beta$ 4-10) (Figure 6(a)).

**GLUT-1 staining.** All brains were processed for immunohistochemical staining with GLUT-1 antibody. In order to reveal the changes in total amount of GLUT-1, we measured the relative area of the total section area being stained for GLUT-1 in the cortex, hippocampus, and thalamus (Figure 6(b)). While in the cortical and hippocampal regions, no effects were detected, all AngII-infused animals displayed increased GLUT-1 in the thalamus compared to their Sal-infused littermates ( $F(1,22) = 3.4$ ,  $p = 0.039$ ).

Only in thalamic regions of all Sal-infused mice, EM treatment increased amount of GLUT-1 ( $F(1,20) = 5.3$ ,  $p = 0.032$ ).

We also measured vascular density via the number of GLUT-1+ bloodvessels, but no significant effects were found (data not shown).

**IBA-1 staining.** The brains of all mice were immunohistochemically stained for IBA-1. IBA-1 is specifically expressed in activated microglia. The typical example of the combined picture of Figure 6(a) demonstrates clearly the colocalisation of IBA-1 with A $\beta$ . We measured relative area of the total section area being stained for IBA-1 in the cortex, hippocampus, and thalamus as measure for amount of activated microglia (Figure 6(c)).

No significant results were found for the amount of activated microglia.

**$\beta$ -Amyloid staining.** The brains of all A $\beta$ PP/PS1 mice were immunohistochemically stained with WO-2 antibody. As previously shown, brains of WT mice showed no immunoreactivity with this antibody,<sup>76</sup> while A $\beta$  deposits in transgenic mice were intensively stained. We measured the relative area of the total section area covered with A $\beta$  depositions in the cortex, hippocampus, and thalamus (Figure 6(d)).

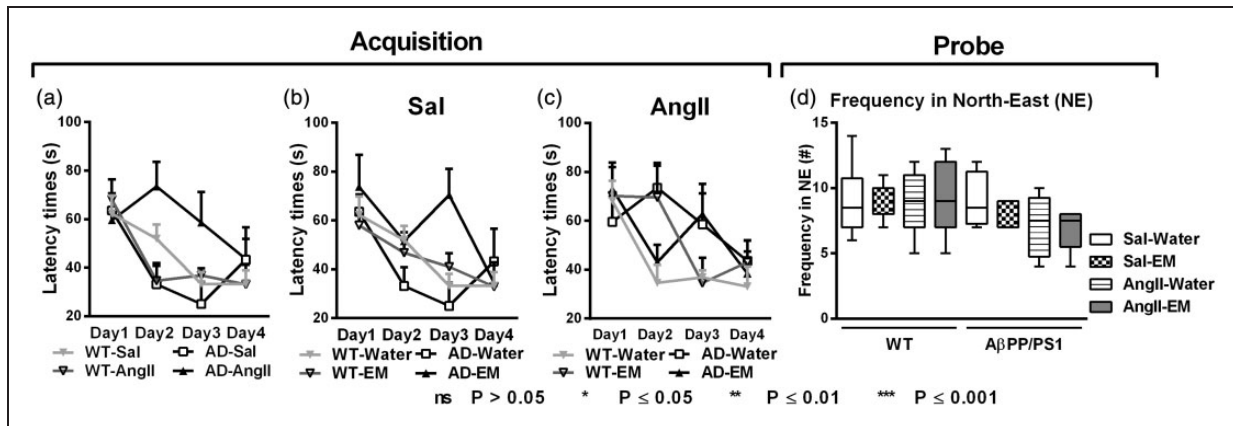


**Figure 5.** Analysed data of the Morris water maze (MWM) performed by 11-month-old Sal-infused (saline) and AngII-infused (angiotensin II) A $\beta$ PP/PS1 (Alzheimer's disease, AD) and wild-type (WT) mice, treated with eprosartan mesylate (EM) vs. normal drinking water as control. While during task acquisition, all mice were trained in the MWM to assess spatial learning capabilities during 11 month of age (a+b+c); during the probe phase, the ability to remember the former platform location in the pool area was measured using the frequency of crossing NE quadrant of the pool area containing the platform location was measured as probe trial performance (d). (a) Task acquisition performance revealed that in untreated mice (no EM) almost all animal groups, Sal-infused WT mice ( $p = 0.006$ ), Sal-infused A $\beta$ PP/PS1 mice ( $p = 0.041$ ), and AngII-infused WT mice ( $p = 0.005$ ), were able to learn to find the platform from acquisition day 1 to day 4, except of the AngII-infused A $\beta$ PP/PS1 mice. This latter experimental group could not learn to find the platform from acquisition day 1 to day 4 ( $p = 0.100$ ). (b+c) Combining EM-treated with untreated mice revealed no effect nor a genotype by antihypertensive treatment interaction. (d) During the probe trial of the MWM, the ability to cross NE quadrant of the pool area containing the platform location was measured as probe trial performance indicating spatial memory capacity. No effect on spatial memory was found.

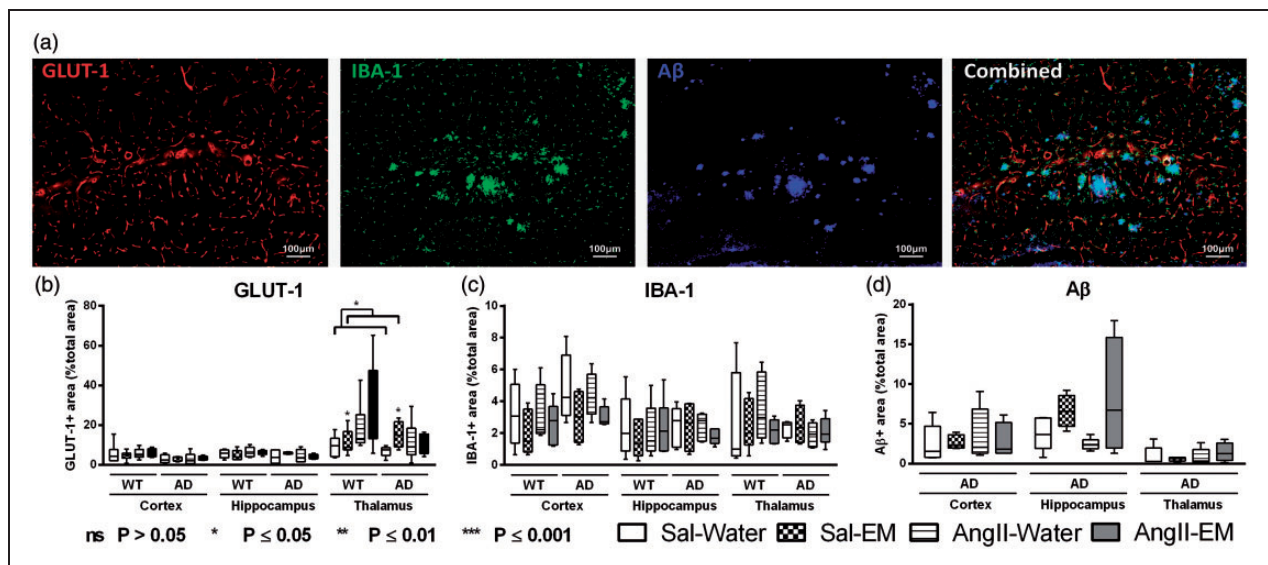


**Figure 6.** Distribution of glucose transporter-1 (GLUT-1), ionised calcium-binding adapter molecule 1 (IBA-1), and amyloid- $\beta$  (A $\beta$ ) in the cortex, hippocampus, and thalamus of 12-month-old Sal-infused (saline) and AngII-infused (Angiotensin II) A $\beta$ PP/PS1 (Alzheimer's disease, AD) and wild-type (WT) mice, treated with eprosartan mesylate (EM) vs. normal drinking water as control. A representative example of vessel density (GLUT-1), neuroinflammation (IBA-1), A $\beta$  staining, and an overlay of all three staining in an A $\beta$ PP/PS1 mouse is shown (a). (b) The brains of all mice underwent immunohistochemical staining with GLUT-1 antibody representing amount of GLUT-1. While in the cortical and hippocampal regions, no effect was detected, all AngII-infused animals displayed an increased amount of GLUT-1 in the thalamus compared to their Sal-infused littermates ( $p = 0.039$ ). Only in thalamic regions of all Sal-infused mice, EM treatment increased amount of GLUT-1 ( $p = 0.032$ ). (c) The brains of all mice were immunohistochemically stained with an antibody against IBA-1 being specifically expressed in activated microglia. Notably, A $\beta$  and microglia are colocalised as demonstrated in the combined picture. No significant differences were found for IBA-1. (d) The brains of all A $\beta$ PP/PS1 mice were immunohistochemically stained with WO-2/A $\beta$  antibody (mouse anti-human A $\beta$ 4-10). No significant AngII- or antihypertensive treatment effects were found.

**Table 1.** Summary of all significant results.

Parameter		Results	
Body weight			
Drinking behaviour		↑ in AngII-infused mice	
SBP	Aging	↑ in AngII-infused mice	
	12-Month	↑ in AngII-infused mice; ↑ in AD mice; ↓ in AngII-infused mice on EM	
CBF	Cortex	↓ in AD mice	
	Hippocampus	↑ in mice on EM	
	Thalamus		
DTI	FA	Auditory cortex	
		Corpus callosum	
		Fornix	
		Hippocampus	↑ in AngII-infused animals on EM
		Motor cortex	
		Optic tract	↑ in AngII-infused animals on EM
		Somatosensory cortex	
	MD	Auditory cortex	
		Corpus callosum	
		Fornix	
		Hippocampus	
		Motor cortex	↓ in Sal-infused mice on EM; ↓ in AngII-infused AD mice on EM
		Optic tract	↓ in AngII-infused WT mice on EM
		Somatosensory cortex	
Visual cortex			
rsfMRI	Total correlations	↓ in AngII-infused mice; ↓ in Sal-infused mice on EM; ↑ in AngII-infused mice on EM	
MWM	Acquisition	Latency times	
	Probe	# NE-quadrant	↓ spatial learning in AngII-infused AD mice
IHC	GLUT-1		↑ in thalamus of AngII-infused mice; ↑ in thalamus of mice on EM
	IBA-1		
	A $\beta$		

AngII: Angiotensin II; AD: Alzheimer's disease; SBP: systolic blood pressure; EM: eprosartan mesylate; CBF: cerebral blood flow; DTI: diffusion tensor imaging; FA: fractional anisotropy; MD: mean diffusivity; Sal: saline; rsfMRI: resting-state functional MRI; Total: total correlations; partial: partial correlations; MWM: Morris water maze; NE: north-east; GLUT-1: glucose transporter-1; IBA-1: ionised calcium-binding adapter molecule 1; A $\beta$ : amyloid- $\beta$ .

No significant results were found for the area covered with A $\beta$  depositions in the cortex, hippocampus, and thalamus.

A summary of all experimental results is given in Table 1.

## Discussion

This study assessed the potential relationships between angiotensin-II-induced hypertension and AD-related cerebrovascular, metabolic, connectivity, and cognitive changes in a mouse model for AD and WT controls. A

summary of all significant results can be found in Table 1.

We found that AngII-induced hypertension did not induce a total AD pathology in WT mice. One explanation for these results could be the use of relatively young mice. In accordance, Toth et al.<sup>77</sup> showed that aging impairs autoregulatory protection in the brain, and this aggravates potentially cerebrovascular injury and neuroinflammation.

However, AngII led to a reduced FC in these WT mice, see supplementary Table 2. In clinical studies, a decreased FC was found in AD patients.<sup>78–80</sup>

In support, a preclinical study using a mouse model for cerebral amyloidosis showed a compromised FC resulting in functional impairments affecting the sensory motor cortex already in pre-plaque stage.<sup>81</sup> In the current study, we showed that in a hypertension model a reduction in FC could be introduced via AngII-induced hypertension, in absence of classical AD pathology (amyloidosis). A limitation of the acquired FC results is that the rsfMRI measurements are performed in isoflurane anaesthetised mice. Fortunately, in both pre-clinical and clinical studies using rsfMRI, a general structure of the functional networks transcending levels of consciousness was detected.<sup>82–84</sup> Zhou et al.<sup>85</sup> and Liang et al.<sup>86</sup> have confirmed the presence of a bilateral cortical connectivity in several cortical regions also under isoflurane anaesthesia. Nevertheless, in isoflurane anaesthetised mice Jonckers et al.<sup>87</sup> and Guilfoyle et al.<sup>88</sup> did not find the same level of bilateral connectivity. However, in our previous and recent studies using isoflurane as anaesthesia, we confirmed the presence of networks in several well-defined cortical and subcortical brain regions in two different murine models for vascular risk factors for AD.<sup>65,89</sup> In our previous work, we confirmed that both FC and CBF are dependent on isoflurane concentrations, and both FC and CBF decline with concentrations of isoflurane >2.2%, but do not further decline below a concentration of 2.2%.<sup>90</sup> Therefore, using the low-dose isoflurane (~1.7%) in this recent experiment will preserve the resting-state networks and will not interfere with the outcome of this study, as all animals were kept under the same low isoflurane concentration.

Second, we used an AD mouse model to study the influence of AngII-induced hypertension on AD pathology. As expected, in all mice (AD and WT), AngII increased SBP. This result is in line with other studies showing that AngII causes vasoconstriction and increased BP by binding to AT1 and AT2 receptors.<sup>16,17,67</sup> However, at 12 months of age, our AD mice had a higher SBP than their WT littermates, confirming recent findings.<sup>63</sup> Our results revealed a relationship between aging, AngII-induced hypertension and Alzheimer-like (A $\beta$ -overexpression) pathology leading to an increased SBP. A possible explanation for this finding is that A $\beta$  enhances the vasoconstrictive effect of AngII, or causes vasoconstriction independent of AngII. Niwa et al.<sup>26</sup> have shown that A $\beta$  acts directly on cerebral arteries to enhance vasoconstriction and to stimulate selected constrictor responses, resulting in a reduced CBF. In accordance, we showed that our AD mice showed also an impaired CBF, similar to our earlier study in the same AD mouse model.<sup>66</sup> Studies in patients with mild cognitive impairment (MCI) and AD patients also identified a significant reduction in regional and global CBF.<sup>90</sup> Whether this reduction is due to

reduced metabolic demand or due to vascular pathology is difficult to disentangle in human studies. Contrarily to our expectations, we could not detect hypertension-induced overexpression of A $\beta$  in the cortex, hippocampus nor thalamus in the brains of the AD-like mice, while these mice do show impaired cortical CBF. Sun et al.<sup>91</sup> induced hypoxia, a direct consequence of hypoperfusion, in another A $\beta$  overexpressing mouse model at eight months of age and revealed both an increased A $\beta$  deposition and neuritic plaque formation, whereas in our study hypertension was induced by AngII-infusion for only 2 months starting from 10 months of age. A limitation of this study is the usage of a relatively high dosage (500 ng·kg<sup>-1</sup>·min<sup>-1</sup>) of AngII being infused via osmotic minipumps for 2 months starting from 10 months of age. Using this hypertension model, we wanted to simulate hypertension during mid-life via chronically elevated levels of AngII for only two months. Therefore, we needed a slightly higher dosage of AngII increasing SBP already after a short period of time to induce AngII-induced hypertension and the consequent pathological changes resembling the human situation. For example, the Honolulu Asia Aging Study revealed that untreated hypertension during mid-life can increase the risk for late age dementia in men.<sup>7</sup> Dosages of 200 ng·kg<sup>-1</sup>·min<sup>-1</sup> and 400 ng·kg<sup>-1</sup>·min<sup>-1</sup> using the same slow pressor model have proven not to elevate SBP within the first six days after the implantation of the osmotic minipumps, while a dosage of 1.000 ng·kg<sup>-1</sup>·min<sup>-1</sup> heightened SBP already at three days after the implantation.<sup>92</sup> However, Qi et al.<sup>93</sup> also infused six-week-old mice via osmotic minipumps with even a higher dosage of AngII (1.500 ng·kg<sup>-1</sup>·min<sup>-1</sup>) for seven days increasing SBP already at four days post operation. Nevertheless, Edgley et al.<sup>94</sup> have proven that intravenous infusions of AngII into the systemic circulation require much lower dosages of AngII.

In summary, our AD mice exhibited an increased SBP and a decreased cortical CBF. In addition, AD mice on AngII showed a decreased FC like their WT littermates, but only in these AngII-infused AD mice did this lead to a lowered spatial learning capacity. RsfMRI has developed into a method for the analysis of spontaneous neural activity through the BOLD signal change<sup>95</sup> representing FC. Our findings indicating an impaired FC in AngII-infused mice are in line with a recent study that found reduced connectivity in cortex regions of older hypertensive AD patients relative to older non-hypertensive AD patients.<sup>96</sup> We found no cognitive effects of AngII-induced hypertension in WT animals. Haley et al.<sup>97</sup> demonstrated even in healthy young adults that a family history of hypertension was associated with subtle changes in visuospatial attention combined with a lowered task-related

activation in several brain regions during this visuospatial working memory task. This result is in accordance with a study revealing an impaired memory and learning in hypertensive rats.<sup>98</sup> Hypertensive patients had deficits in the WM and FC in frontal and parietal lobes, associated with cognitive decline.<sup>99</sup> However, only our AngII-infused AD model mice exhibited a decreased spatial learning capacity during the MWM, which could be due to the functional connective impairments combined with the loss of cortical CBF being only present in this experimental group.

We could not observe genotype or AngII effects on structural connectivity. In this study, AngII-infusion was administered only for 2 months starting from 10 months of age. This short duration of AngII-infusion could be one reason; we found no changes in structural connectivity measured via DTI. Another explanation could be the increased amount of GLUT-1 measured in the thalamus of AngII-infused mice as a compensatory mechanism. GLUT-1 is responsible for the transfer of glucose across the blood–brain barrier and being selectively expressed at high levels in the capillary endothelium of the brain.<sup>30</sup> GLUT-1 is a marker for vascular endothelial cells and cerebral metabolism. In several animal studies, myocardial ischemia increased the synthesis of GLUT-1 mRNA and protein levels in both ischemic and also nonischemic cardiac regions indicating also a potential rescue mechanism for myocardial ischemia.<sup>100,101</sup> Notably, McCall et al.<sup>102</sup> reported an overexpression of GLUT-1 in microvessels after the onset of global cerebral ischemia in the rat brain. Moreover, Urabe et al.<sup>103</sup> and Gerhart et al.<sup>104</sup> also showed also an overexpression of GLUT-1 in the cerebral cortex in two ischemia and reperfusion animal models. However, no effects of genotype or AngII-infusion were found on vascular density.

In summary, regarding our second aim of this study, AD model mice had an increased SBP and an impaired CBF. Furthermore, AngII-induced hypertension exacerbated several AD-like pathological changes such as impaired CBF, impaired FC, and cognitive impairment. These results are in accordance with the recent study of Cifuentes et al.<sup>105</sup> demonstrating that hypertension advances the development of AD-like structural and functional alterations, partially through cerebral vasculature impairment and reduced nitric oxide production. This result of Cifuentes et al. is in line with our results of the immunohistochemical data of IBA-1, a marker for activated microglia.<sup>37–39</sup> Here, no differences in amount of IBA-1+ cells nor immunohistochemically stained surface in the AngII-infused and AD model mice could be observed.

Another aim of this study was to investigate the effect of an ARB such as EM on possible (neuro) pathological changes induced by hypertension and to

indicate a relationship between the AD-like pathology, AngII, and its receptors.

In all AngII-infused experimental mice, treatment with the angiotensin-receptor blocker EM restored SBP, in line with previous work.<sup>106</sup> Treatment of hypertension with EM enhanced hippocampal CBF. This beneficial effect was shown in all mice and was not restricted to transgenic animals only, indicating that either BP lowering or blocking effects of endogenous AngII may be beneficial for brain perfusion. In accordance, Tryambake et al.<sup>107</sup> demonstrated that BP lowering treatments increased CBF in older subjects with hypertension as well.

A beneficial effect of EM was detected in all AngII-infused mice regarding the structural connectivity. Here, FA in the hippocampus and optic tract was increased in EM-treated AngII-infused mice indicating an improved microstructural integrity, while after EM treatment MD of the motor cortex of Sal-infused mice and of AngII-infused AD mice, and MD of the optic tract of AngII-infused WT mice was lowered. In accordance, Gons et al.<sup>108</sup> showed that increased BP is associated with a decrease in FA respectively an increase in MD. De Leeuw et al.<sup>109</sup> also demonstrated that long-standing hypertension increases the risk of developing WM lesions. Notably, a novel finding is the negative effect of EM on FC in all Sal-infused mice, but not in AngII-infused mice, see supplementary Table 2 for a detailed description of the significant results. While all Sal-infused EM-treated mice showed a decreased FC compared with untreated mice, all AngII-infused EM-treated mice showed an increased FC compared with untreated mice. In addition, Füchtmeier et al.<sup>110</sup> showed that Compound 21, an AngII receptor type 2 agonist, had opposing effects on spatial reference memory in hypoperfused and sham mice. These effects need to be further investigated in future studies but suggest that blockade of the AngII receptors in absence of elevated AngII levels may have harmful effects on structural connectivity and cognition. Moreover, Henriksen et al.<sup>111</sup> also showed in insulin resistant obese Zucker rats that irbesartan, another AngII receptor antagonist, improved insulin sensitivity and glucose tolerance in the skeletal muscle by increasing the protein expression of GLUT 4, indicating the importance of measuring insulin and glucose blood levels and the relationship with AngII in future studies. Furthermore, it will be interesting to investigate the possible role of phosphorylated tau (pTau) in follow-up studies, because of the emerging role of pTau in pathology and behaviour for both AD.<sup>112</sup> Glózik et al.<sup>113</sup> revealed that only in hypertensive subjects a longitudinal decrease in mean arterial pressure was related to memory decline and an increase in phosphorylated tau. Another interesting aspect to

investigate in future studies is how hypertension affects heart hypertrophy, and whether cognitive decline and decreased connectivity are indirect effects of heart diseases. In a systematic review, Vogels et al.<sup>114</sup> confirmed that heart failure is associated with a pattern of generalised cognitive impairment that includes primarily memory, attention, mental flexibility, and global cognitive deficits.

In conclusion, we showed that chronic infusion of AngII increased SBP in both transgenic and WT mice, which could be reversed by EM treatment. In addition, aging combined with AD pathology exacerbated the increase in SBP. Correspondingly, cerebral perfusion was impaired in the AD mouse model.

Furthermore, EM treatment improved the WM integrity combined with increased CBF and improved FC. AngII-induced hypertension impaired the FC in AD and WT mice comparably, indicating a negative role of hypertension on FC irrespective of AD pathology.

Our results suggest that elevated levels of AngII may indeed represent a mechanistic link between the risk factor hypertension and the clinical development of AD; however, AngII may not to be a causal factor for sporadic AD as it did not initiate amyloid pathology in this study. Rather, it may progress the clinical development of AD in people with amyloid accumulation through its negative effects on CBF, FC, and cognition. Recent human studies on sporadic AD indicate that amyloid accumulation increases with age to as much as 30%–50% of the normal population over the age of 70, but can remain asymptomatic for decades.<sup>115–117</sup> We speculate that elevated levels of AngII (essential hypertension) may be a factor promoting the development of symptomatic disease. In addition, our study suggests that elevated AngII may also lead to abnormalities that may mimic AD (reduced FC leading to cognitive decline) which could imply that hypertension may lead to dementia that has similarity with AD and may be clinically diagnosed as such. In both scenarios, however, counteracting the negative effects of elevated AngII will have a beneficial effect in reducing the prevalence of dementia. Gathering more insight in the actions of antihypertensive treatments on brain processes and the vascular system could support the development of effective tailor-made BP-lowering treatments for AD patients.

### Funding

The author(s) disclosed receipt of the following financial support for the research, authorship, and/or publication of this article: This study was supported by a grant (no11528) from the Internationale Stichting Alzheimer Onderzoek (ISAO) and the EU 7th framework LipidiDiet project (FP7/2007-2013) under grant agreement no211696.

### Acknowledgements

We would like to thank Bianca Lemmers-van de Weem, Kitty Lemmens-Hermans, Iris Lamers-Elementans, Karin de Haas-Cremers, and Henk Arnts for their excellent care for our mice.

### Declaration of conflicting interests

The author(s) declared no potential conflicts of interest with respect to the research, authorship, and/or publication of this article.

### Authors' contributions

MW, AJK, and JAHRC designed research; MW, MR, and RvdL performed research; MW, MR, and RvdL analysed data; MW, AJK, and JAHRC wrote the paper; and AH, AJK, and JAHRC made critical revision.

### Supplementary material

Supplementary material for this paper can be found at <http://jcbfm.sagepub.com/content/by/supplemental-data>

### References

1. Wimo A, Winblad B and Jönsson L. The worldwide societal costs of dementia: estimates for 2009. *Alzheimers Dement* 2010; 6: 98–103.
2. Arevalo-Rodriguez I, Pedraza OL, Rodríguez A, et al. Alzheimer's disease dementia guidelines for diagnostic testing: a systematic review. *Am J Alzheimers Dis Other Demen* 2013; 28: 111–119.
3. Morris JC. The nosology of dementia. *Neurol Clin* 2000; 18: 773–788.
4. Iadecola C and Gorelick PB. Converging pathogenic mechanisms in vascular and neurodegenerative dementia. *Stroke* 2003; 34: 335–337.
5. Kilander L, Andrén B, Nyman H, et al. Atrial fibrillation is an independent determinant of low cognitive function. *Stroke* 1998; 29: 1816–1820.
6. Kivipelto M, Helkala E-L, Laakso MP, et al. Midlife vascular risk factors and Alzheimer's disease in later life: longitudinal, population based study. *BMJ* 2001; 322: 1447–1451.
7. Launer LJ, Ross GW, Petrovitch H, et al. Midlife blood pressure and dementia: the Honolulu–Asia aging study. *Neurobiol Aging* 2000; 21: 49–55.
8. Nagata KEN, Sato M, Satoh Y, et al. Hemodynamic aspects of Alzheimer's disease. *Ann N Y Acad Sci* 2002; 977: 391–402.
9. Ott A, Stolk RP, Hofman A, et al. Association of diabetes mellitus and dementia: the Rotterdam study. *Diabetologia* 1996; 39: 1392–1397.
10. Posner HB, Tang M-X, Luchsinger J, et al. The relationship of hypertension in the elderly to AD, vascular dementia, and cognitive function. *Neurology* 2000; 58: 1175–1181.
11. Ringman JM, Sachs MC, Zhou Y, et al. Clinical predictors of severe cerebral amyloid angiopathy and influence of apoe genotype in persons with pathologically

- verified Alzheimer disease. *JAMA Neurol* 2014; 71: 878–883.
12. Wiesmann M, Kiliaan AJ and Claassen JA. Vascular aspects of cognitive impairment and dementia. *J Cereb Blood Flow Metab* 2013; 33: 1696–1706.
  13. Skoog I, Nilsson L, Persson G, et al. 15-year longitudinal study of blood pressure and dementia. *Lancet* 1996; 347: 1141–1145.
  14. Hofman A, Ott A, Breteler M, et al. Atherosclerosis, apolipoprotein E, and prevalence of dementia and Alzheimer's disease in the Rotterdam Study. *Lancet* 1997; 349: 151–154.
  15. Kehoe PG and Wilcock GK. Is inhibition of the renin-angiotensin system a new treatment option for Alzheimer's disease? *Lancet Neurol* 2007; 6: 373–378.
  16. Brasier AR, Recinos A and Eledrisi MS. Vascular inflammation and the renin-angiotensin system. *Arterioscler Thromb Vasc Biol* 2002; 22: 1257–1266.
  17. Kehoe PG, Miners S and Love S. Angiotensins in Alzheimer's disease—friend or foe? *Trends Neurosci* 2009; 32: 619–628.
  18. Reckelhoff JF and Romero JC. Role of oxidative stress in angiotensin-induced hypertension. *Am J Physiol Regul Integr Comp Physiol* 2003; 284: R893–R912.
  19. Bloch S, Obari D and Girouard H. Angiotensin and neurovascular coupling: beyond hypertension. *Microcirculation* 2015; 22: 159–167.
  20. Saavedra JM. Brain angiotensin II: new developments, unanswered questions and therapeutic opportunities. *Cell Mol Neurobiol* 2005; 25: 485–512.
  21. Marchesi C, Paradis P and Schiffrin EL. Role of the renin-angiotensin system in vascular inflammation. *Trends Pharmacol Sci* 2008; 29: 367–374.
  22. Gorelick PB, Scuteri A, Black SE, et al. Vascular contributions to cognitive impairment and dementia a statement for healthcare professionals from the American Heart Association/American Stroke Association. *Stroke* 2011; 42: 2672–2713.
  23. Kurinami H, Shimamura M, Sato N, et al. Do angiotensin receptor blockers protect against Alzheimer's disease? *Drugs Aging* 2013; 30: 1–6.
  24. Capone C, Faraco G, Park L, et al. The cerebrovascular dysfunction induced by slow pressor doses of angiotensin II precedes the development of hypertension. *Am J Physiol Heart Circ Physiol* 2011; 300: H397–H407.
  25. Ruitenbergh A, den Heijer T, Bakker SLM, et al. Cerebral hypoperfusion and clinical onset of dementia: the Rotterdam study. *Ann Neurol* 2005; 57: 789–794.
  26. Niwa K, Porter VA, Kazama K, et al. A $\beta$ -peptides enhance vasoconstriction in cerebral circulation. *Am J Physiol Heart Circ Physiol* 2001; 281: H2417–H2424.
  27. Prohovnik I, Mayeux R, Sackeim HA, et al. Cerebral perfusion as a diagnostic marker of early Alzheimer's disease. *Neurology* 1988; 38: 931.
  28. Duara R, Grady C, Haxby J, et al. Positron emission tomography in Alzheimer's disease. *Neurology* 1986; 36: 879.
  29. Jagust WJ, Seab JP, Huesman RH, et al. Diminished glucose transport in Alzheimer's disease: dynamic PET studies. *J Cereb Blood Flow Metab* 1991; 11: 323–330.
  30. Choeiri C, Staines W and Messier C. Immunohistochemical localization and quantification of glucose transporters in the mouse brain. *Neuroscience* 2002; 111: 19–34.
  31. Simpson IA, Chundu KR, Davies-Hill T, et al. Decreased concentrations of GLUT1 and GLUT3 glucose transporters in the brains of patients with Alzheimer's disease. *Ann Neurol* 1994; 35: 546–551.
  32. Kalara RN and Harik SI. Reduced glucose transporter at the blood-brain barrier and in cerebral cortex in Alzheimer disease. *J Neurochem* 1989; 53: 1083–1088.
  33. Horwood N and Davies DC. Immunolabelling of hippocampal microvessel glucose transporter protein is reduced in Alzheimer's disease. *Virchows Arch* 1994; 425: 69–72.
  34. Akiyama H, Barger S, Barnum S, et al. Inflammation and Alzheimer's disease. *Neurobiol Aging* 2000; 21: 383–421.
  35. Perry VH, Cunningham C and Holmes C. Systemic infections and inflammation affect chronic neurodegeneration. *Nat Rev Immunol* 2007; 7: 161–167.
  36. Zotova E, Nicoll JA, Kalara R, et al. Inflammation in Alzheimer's disease: relevance to pathogenesis and therapy. *Alzheimers Res Ther* 2010; 2: 1–9.
  37. Imai Y, Ibata I, Ito D, et al. A novel gene *iba1* in the major histocompatibility complex class III region encoding an EF hand protein expressed in a monocytic lineage. *Biochem Biophys Res Commun* 1996; 224: 855–862.
  38. Ahmed Z, Shaw G, Sharma VP, et al. Actin-binding proteins coronin-1a and IBA-1 are effective microglial markers for immunohistochemistry. *J Histochem Cytochem* 2007; 55: 687–700.
  39. Streit WJ, Braak H, Xue Q-S, et al. Dystrophic (senescent) rather than activated microglial cells are associated with tau pathology and likely precede neurodegeneration in Alzheimer's disease. *Acta Neuropathol* 2009; 118: 475–485.
  40. Yamada K, Uchida S, Takahashi S, et al. Effect of a centrally active angiotensin-converting enzyme inhibitor, perindopril, on cognitive performance in a mouse model of Alzheimer's disease. *Brain Res* 2010; 1352: 176–186.
  41. Muller M, van der Graaf Y, Visseren FL, et al. Hypertension and longitudinal changes in cerebral blood flow: the SMART-MR study. *Ann Neurol* 2012; 71: 825–833.
  42. Tsukuda K, Mogi M, Iwanami J, et al. Cognitive deficit in amyloid- $\beta$ -injected mice was improved by pretreatment with a low dose of telmisartan partly because of peroxisome proliferator-activated receptor- $\gamma$  activation. *Hypertension* 2009; 54: 782–787.
  43. Shlyakhto E. Observational Study on Cognitive function And systolic blood pressure Reduction (OSCAR): preliminary analysis of 6-month data from > 10000 patients and review of the literature. *Curr Med Res Opin* 2007; 23: S13–S18.
  44. Haag M, Hofman A, Koudstaal P, et al. Duration of antihypertensive drug use and risk of dementia A prospective cohort study. *Neurology* 2009; 72: 1727–1734.
  45. Keeman J, Mazel J and Zitman F. *Het medisch jaar 2008/2009*. Houten, The Netherlands: Bohn Stafleu van Loghum, 2009.
  46. Davies NM, Kehoe PG, Ben-Shlomo Y, et al. Associations of anti-hypertensive treatments with

- Alzheimer's disease, vascular dementia, and other dementias. *J Alzheimers Dis* 2011; 26: 699–708.
47. Marpillat NL, Macquin-Mavier I, Tropeano A-I, et al. Antihypertensive classes, cognitive decline and incidence of dementia: a network meta-analysis. *J Hypertens* 2013; 31: 1073–1082.
  48. Zimmerman MC, Lazartigues E, Sharma RV, et al. Hypertension caused by angiotensin II infusion involves increased superoxide production in the central nervous system. *Circ Res* 2004; 95: 210–216.
  49. Alsop DC, Detre JA and Grossman M. Assessment of cerebral blood flow in Alzheimer's disease by spin-labeled magnetic resonance imaging. *Ann Neurol* 2000; 47: 93–100.
  50. Sandson TA, O'Connor M, Sperling RA, et al. Noninvasive perfusion MRI in Alzheimer's disease: a preliminary report. *Neurology* 1996; 47: 1339–1342.
  51. Asllani I, Habeck C, Scarmeas N, et al. Multivariate and univariate analysis of continuous arterial spin labeling perfusion MRI in Alzheimer's disease. *J Cereb Blood Flow Metab* 2008; 28: 725–736.
  52. Stebbins GT and Murphy CM. Diffusion tensor imaging in Alzheimer's disease and mild cognitive impairment. *Behav Neurol* 2009; 21: 39–49.
  53. Salat DH, Tuch DS, van der Kouwe AJW, et al. White matter pathology isolates the hippocampal formation in Alzheimer's disease. *Neurobiol Aging* 2010; 31: 244–256.
  54. Bozzali M, Falini A, Franceschi M, et al. White matter damage in Alzheimer's disease assessed in vivo using diffusion tensor magnetic resonance imaging. *J Neurol Neurosurg Psychiatry* 2002; 72: 742–746.
  55. Stahl R, Dietrich O, Teipel SJ, et al. White matter damage in Alzheimer disease and mild cognitive impairment: assessment with diffusion-tensor MR imaging and parallel imaging techniques. *Radiology* 2007; 243: 483–492.
  56. Head D, Buckner RL, Shimony JS, et al. Differential vulnerability of anterior white matter in nondemented aging with minimal acceleration in dementia of the Alzheimer type: evidence from diffusion tensor imaging. *Cereb Cortex* 2004; 14: 410–423.
  57. Fellgiebel A, Wille P, Müller MJ, et al. Ultrastructural hippocampal and white matter alterations in mild cognitive impairment: a diffusion tensor imaging study. *Dement Geriatr Cogn Disord* 2004; 18: 101–108.
  58. Bozzali M, Franceschi M, Falini A, et al. Quantification of tissue damage in AD using diffusion tensor and magnetization transfer MRI. *Neurology* 2001; 57: 1135–1137.
  59. Kavcic V, Ni H, Zhu T, et al. White matter integrity linked to functional impairments in aging and early Alzheimer's disease. *Alzheimers Dement* 2008; 4: 381–389.
  60. Jankowsky JL, Fadale DJ, Anderson J, et al. Mutant presenilins specifically elevate the levels of the 42 residue  $\beta$ -amyloid peptide in vivo: evidence for augmentation of a 42-specific  $\gamma$  secretase. *Hum Mol Genet* 2004; 13: 159–170.
  61. Jankowsky JL, Slunt HH, Ratovitski T, et al. Co-expression of multiple transgenes in mouse CNS: a comparison of strategies. *Biomol Eng* 2001; 17: 157–165.
  62. Kilkenny C, Browne WJ, Cuthill IC, et al. Improving bioscience research reporting: the ARRIVE guidelines for reporting animal research. *PLoS Biol* 2010; 8: e1000412.
  63. Wiesmann M, Capone C, Zerbi V, et al. Hypertension impairs cerebral blood flow in a mouse model for Alzheimer's disease. *Curr Alzheimer Res* 2015; 12: 914–922.
  64. Janssen CIF, Zerbi V, Mutsaers MPC, et al. Impact of dietary n-3 polyunsaturated fatty acids on cognition, motor skills and hippocampal neurogenesis in developing C57BL/6J mice. *J Nutr Biochem* 2015; 26: 24–35.
  65. Wiesmann M, Zerbi V, Jansen D, et al. A dietary treatment improves cerebral blood flow and brain connectivity in aging apoE4 mice. *Neural Plast* 2016; 2016: 15.
  66. Zerbi V, Jansen D, Wiesmann M, et al. Multinutrient diets improve cerebral perfusion and neuroprotection in a murine model of Alzheimer's disease. *Neurobiol Aging* 2014; 35: 600–613.
  67. Kim SG. Quantification of relative cerebral blood flow change by flow-sensitive alternating inversion recovery (FAIR) technique: Application to functional mapping. *Magn Reson Med* 1995; 34: 293–301.
  68. Kwong KK, Chesler DA, Weisskoff RM, et al. MR perfusion studies with T1-weighted echo planar imaging. *Magn Reson Med* 1995; 34: 878–887.
  69. Paxinos G and Franklin KB. *The mouse brain in stereotaxic coordinates*/George Paxinos, Keith Franklin. London: Academic, 2004.
  70. Harsan LA, Paul D, Schnell S, et al. In vivo diffusion tensor magnetic resonance imaging and fiber tracking of the mouse brain. *NMR Biomed* 2010; 23: 884–896.
  71. Jansen D, Zerbi V, Janssen CI, et al. Impact of a multi-nutrient diet on cognition, brain metabolism, hemodynamics, and plasticity in apoE4 carrier and apoE knockout mice. *Brain Struct Funct* 2014; 219: 1841–1868.
  72. Le Bihan D, Mangin J-F, Poupon C, et al. Diffusion tensor imaging: concepts and applications. *J Magn Reson Imaging* 2001; 13: 534–546.
  73. Alexander AL, Hurley SA, Samsonov AA, et al. Characterization of cerebral white matter properties using quantitative magnetic resonance imaging stains. *Brain Connect* 2011; 1: 423–446.
  74. Feldman HM, Yeatman JD, Lee ES, et al. Diffusion tensor imaging: a review for pediatric researchers and clinicians. *J Dev Behav Pediatr* 2010; 31: 346–356.
  75. Li R, Wu X, Chen K, et al. Alterations of directional connectivity among resting-state networks in Alzheimer disease. *AJNR Am J Neuroradiol* 2013; 34: 340–345.
  76. Hooijmans CR, Graven C, Dederen PJ, et al. Amyloid beta deposition is related to decreased glucose transporter-1 levels and hippocampal atrophy in brains of aged APP/PS1 mice. *Brain Res* 2007; 1181: 93–103.
  77. Toth P, Tucsek Z, Sosnowska D, et al. Age-related autoregulatory dysfunction and cerebrovascular injury in mice with angiotensin II-induced hypertension. *J Cereb Blood Flow Metab* 2013; 33: 1732–1742.
  78. Allen G, Barnard H, McColl R, et al. Reduced hippocampal functional connectivity in Alzheimer disease. *Arch Neurol* 2007; 64: 1482–1487.



79. Supekar K, Menon V, Rubin D, et al. Network analysis of intrinsic functional brain connectivity in Alzheimer's disease. *PLoS Comput Biol* 2008; 4: e1000100.
80. Wang L, Zang Y, He Y, et al. Changes in hippocampal connectivity in the early stages of Alzheimer's disease: evidence from resting state fMRI. *Neuroimage* 2006; 31: 496–504.
81. Grandjean J, Schroeter A, He P, et al. Early alterations in functional connectivity and white matter structure in a transgenic mouse model of cerebral amyloidosis. *J Neurosci* 2014; 34: 13780–13789.
82. Vincent JL, Patel GH, Fox MD, et al. Intrinsic functional architecture in the anaesthetized monkey brain. *Nature* 2007; 447: 83–86.
83. Lu H, Zuo Y, Gu H, et al. Synchronized delta oscillations correlate with the resting-state functional MRI signal. *Proc Natl Acad Sci USA* 2007; 104: 18265–18269.
84. Pan W-J, Billings JCW, Grooms JK, et al. Considerations for resting state functional MRI and functional connectivity studies in rodents. *Front Neurosci* 2015; 9: 269.
85. Zhou IY, Liang Y-X, Chan RW, et al. Brain resting-state functional MRI connectivity: morphological foundation and plasticity. *Neuroimage* 2014; 84: 1–10.
86. Liang Z, King J and Zhang N. Intrinsic organization of the anesthetized brain. *J Neurosci* 2012; 32: 10183–10191.
87. Jonckers E, Van Audekerke J, De Visscher G, et al. Functional connectivity fMRI of the rodent brain: comparison of functional connectivity networks in rat and mouse. *PLoS ONE* 2011; 6: e18876.
88. Guilfoyle DN, Gerum SV, Sanchez JL, et al. Functional connectivity fMRI in mouse brain at 7 T using isoflurane. *J Neurosci Meth* 2013; 214: 144–148.
89. Zerbi V, Wiesmann M, Emmerzaal TL, et al. Resting-state functional connectivity changes in aging apoE4 and apoE-KO mice. *J Neurosci* 2014; 34: 13963–13975.
90. Johnson NA, Jahng G-H, Weiner MW, et al. Pattern of cerebral hypoperfusion in Alzheimer disease and mild cognitive impairment measured with arterial spin-labeling MR imaging: initial experience. *Radiology* 2005; 234: 851–859.
91. Sun X, He G, Qing H, et al. Hypoxia facilitates Alzheimer's disease pathogenesis by up-regulating BACE1 gene expression. *Proc Natl Acad Sci USA* 2006; 103: 18727–18732.
92. Kawada N, Imai E, Karber A, et al. A mouse model of angiotensin II slow pressor response: role of oxidative stress. *J Am Soc Nephrol* 2002; 13: 2860–2868.
93. Qi G, Jia L, Li Y, et al. Angiotensin II infusion-induced inflammation, monocytic fibroblast precursor infiltration, and cardiac fibrosis are pressure dependent. *Cardiovasc Toxicol* 2011; 11: 157–167.
94. Edgley AJ, Kett MM and Anderson WP. 'Slow Pressor' hypertension from low-dose chronic angiotensin II infusion. *Clin Exp Pharmacol Physiol* 2001; 28: 1035–1039.
95. Mantini D, Perrucci MG, Del Gratta C, et al. Electrophysiological signatures of resting state networks in the human brain. *Proc Natl Acad Sci USA* 2007; 104: 13170–13175.
96. Son SJ, Kim J, Lee E, et al. Effect of hypertension on the resting-state functional connectivity in patients with Alzheimer's disease (AD). *Arch Gerontol Geriatr* 2015; 60: 210–216.
97. Haley AP, Gunstad J, Cohen RA, et al. Neural correlates of visuospatial working memory in healthy young adults at risk for hypertension. *Brain Imaging Behav* 2008; 2: 192–199.
98. Sharma B and Singh N. Defensive effect of natrium diethyldithiocarbamate trihydrate (NDDCT) and lisinopril in DOCA-salt hypertension-induced vascular dementia in rats. *Psychopharmacology* 2012; 223: 307–317.
99. Li X, Liang Y, Chen Y, et al. Disrupted frontoparietal network mediates white matter structure dysfunction associated with cognitive decline in hypertension patients. *J Neurosci* 2015; 35: 10015–10024.
100. Brosius FC III, Liu Y, Nguyen N, et al. Persistent myocardial ischemia increases GLUT1 glucose transporter expression in both ischemic and non-ischemic heart regions. *J Mol Cell Cardiol* 1997; 29: 1675–1685.
101. Feldhaus LM and Liedtke AJ. mRNA expression of glycolytic enzymes and glucose transporter proteins in ischemic myocardium with and without reperfusion. *J Mol Cell Cardiol* 1998; 30: 2475–2485.
102. McCall AL, Van Bueren AM, Nipper V, et al. Forebrain ischemia increases glut1 protein in brain microvessels and parenchyma. *J Cereb Blood Flow Metab* 1996; 16: 69–76.
103. Urabe T, Hattori N, Nagamatsu S, et al. Expression of glucose transporters in rat brain following transient focal ischemic injury. *J Neurochem* 1996; 67: 265–271.
104. Gerhart DZ, Leino RL, Taylor WE, et al. GLUT1 and GLUT3 gene expression in gerbil brain following brief ischemia: an in situ hybridization study. *Brain Res Mol Brain Res* 1994; 25: 313–322.
105. Cifuentes D, Poittevin M, Dere E, et al. Hypertension accelerates the progression of Alzheimer-like pathology in a mouse model of the disease. *Hypertension* 2015; 65: 218–224.
106. Derosa G, Ragonesi PD, Mugellini A, et al. Effects of telmisartan compared with eprosartan on blood pressure control, glucose metabolism and lipid profile in hypertensive, type 2 diabetic patients: a randomized, double-blind, placebo-controlled 12-month study. *Hypertens Res* 2004; 27: 457–464.
107. Tryambake D, He J, Firbank MJ, et al. Intensive blood pressure lowering increases cerebral blood flow in older subjects with hypertension. *Hypertension* 2013; 61: 1309–1315.
108. Gons RAR, de Laat KF, van Norden AGW, et al. Hypertension and cerebral diffusion tensor imaging in small vessel disease. *Stroke* 2010; 41: 2801–2806.
109. de Leeuw FE, de Groot JC, Oudkerk M, et al. Hypertension and cerebral white matter lesions in a prospective cohort study. *Brain* 2002; 125: 765–772.
110. Füchtemeier M, Brinckmann MP, Foddiss M, et al. Vascular change and opposing effects of the angiotensin type 2 receptor in a mouse model of vascular cognitive impairment. *J Cereb Blood Flow Metab* 2015; 35: 476–484.
111. Henriksen EJ, Jacob S, Kinnick TR, et al. Selective angiotensin II receptor antagonism reduces insulin

- resistance in obese Zucker rats. *Hypertension* 2001; 38: 884–890.
112. Hampel H, Blennow K, Shaw LM, et al. Total and phosphorylated tau protein as biological markers of Alzheimer's disease. *Exp Gerontol* 2010; 45: 30–40.
  113. Glodzik L, Rusinek H, Pirraglia E, et al. Blood pressure decrease correlates with tau pathology and memory decline in hypertensive elderly. *Neurobiol Aging* 2014; 35: 64–71.
  114. Vogels RLC, Scheltens P, Schroeder-Tanka JM, et al. Cognitive impairment in heart failure: A systematic review of the literature. *Eur J Heart Fail* 2007; 9: 440–449.
  115. Braak H and Del Tredici K. The preclinical phase of the pathological process underlying sporadic Alzheimer's disease. *Brain* 2015; 138: 2814–2833.
  116. Jack CR Jr, Therneau TM, Wiste HJ, et al. Transition rates between amyloid and neurodegeneration biomarker states and to dementia: a population-based, longitudinal cohort study. *Lancet Neurol* 2015; 15: 56–64.
  117. Jack CR Jr, Wiste HJ, Weigand SD, et al. Age-specific population frequencies of cerebral  $\beta$ -amyloidosis and neurodegeneration among people with normal cognitive function aged 50–89 years: a cross-sectional study. *Lancet Neurol* 2014; 13: 997–1005.